BOLETIN DE LA SOCIEDAD ESPAÑOLA DE
Cerámica y Vidrio
www.elsevier.es/bsecv

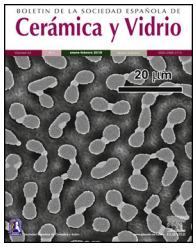

Synthesis and catalytic activity of TiN particles by surfactant-modified urea-glass process

Yohei Saika[a], *Sho Ishiyama*[a], *Nataly Carolina Rosero-Navarro*[b,c,*], *Akira Miura*[b], *Kiyoharu Tadanaga*[b]

[a] *Graduate School of Chemical Sciences and Engineering, Hokkaido University, Sapporo 060-8628, Japan*
[b] *Division of Applied Chemistry, Faculty of Engineering, Hokkaido University, Sapporo 060-8628, Japan*
[c] *Instituto de Cerámica y Vidrio, Madrid 28049, Spain*

ARTICLE INFO

Article history:
Received 18 October 2024
Accepted 26 November 2024
Available online 18 January 2025

Keywords:
TiN
Solution process
Urea
Surfactants
ORR

ABSTRACT

Transition metal nitrides have gained attraction as electrocatalysts of diverse reactions under acid or basic conditions because of their high electric conductivity and excellent chemical stability. The design and control of porous structures are of great interest to enhance their catalytic ability. Herein, the role of a surfactant (triblock copolymer, Pluronic® F127) on the synthesis of titanium nitride by the urea-glass process is investigated. The effect of the surfactant on the catalytic activity is also elucidated. The addition of the surfactant is found to produce a mesostructured TiN with smaller pore diameters and larger pore volume than those without the use of the surfactant. Moreover, the use of the surfactant in the TiN synthesis leads to an improvement of the catalytic activity. Particularly, a four-electron oxygen reduction reaction (ORR) is observed for the TiN prepared by the surfactant-modified urea-glass process.

Síntesis y actividad catalítica de partículas de TiN mediante síntesis de fase líquida modificada con surfactantes

Palabras clave:
TiN
Fase líquida
Urea
Surfactantes
ORR

RESUMEN

Los nitruros de metales de transición son materiales atractivos para su uso como electrocatalizadores de diversas reacciones en condiciones ácidas o básicas debido a su alta conductividad eléctrica y excelente estabilidad química. El diseño y control de estructuras porosas son de gran interés para mejorar su capacidad catalítica. En este trabajo, se investiga la función del uso de un surfactante (copolímero tribloque, Pluronic® F127) en la síntesis de nitruro de titanio por síntesis en fase líquida usando urea. También se dilucida el efecto del

* *Corresponding author.*
E-mail address: rosero@icv.csic.es (N.C. Rosero-Navarro).
https://doi.org/10.1016/j.bsecv.2024.11.002

surfactante en la actividad catalítica. La adición del surfactante produce un TiN mesoestructurado con diámetros de poro más pequeños y un volumen de poro más grande que aquellos sin el uso del surfactante. Además, el uso del surfactante en la síntesis de TiN conduce a una mejora de la actividad catalítica. En particular, se observa una reacción de reducción de oxígeno de cuatro electrones (ORR) para el TiN modificado con surfactante.

Introduction

Transition metal nitrides have been intensively investigated because of their unique properties such as extreme hardness, wear and corrosion resistance, and thermal and electrical properties used in diverse applications, including anticorrosion protective coatings [1,2] and more recently, electrocatalysts and energy conversion and storage [3–5]. Their excellent synergy between electrical properties and chemical stability allows them to be used as electrocatalysts of diverse reactions under acidic or oxidative conditions for fuel cells, batteries or, water splitting [6–8]. Moreover, the transition metal nitrides with a similar *d*-electron density to those of precious metals (*d*-electron density increases by the introduction of nitrogen atoms in the lattice gap) [9] show high catalytic activity, making them a potential and low-cost catalyst alternative. Among them, titanium nitride is of particular interest as catalyst or catalyst support because of its highest electronic conductivity and abundant nature (ninth most abundant element on Earth). Novel applications of titanium nitride include its use as carbon-free cathode material for high energy lithium-oxygen batteries [10], catalyzing the formation and decomposition of Li_2O_2 under nonaqueous conditions or as a catalyst support material for proton exchange membrane fuel cells [11,12], enhancing the catalytic activity of traditional catalyst such as platinum under acidic conditions.

Titanium nitride can be synthesized by the conventional ammonolysis. Generally, ammonolysis can use titanium oxide precursor and then the nitration is carried out under an ammonia flow at temperatures around 700–1100 °C (particle size up to 70 nm) [13]. The urea-glass method has also been used to prepare nitrides [14]. The urea is used as a nitrogen source via a metal-urea complex that further, under heat treatment around 800 °C, results in the formation of titanium nitride nanoparticles (10–20 nm). Recently, considerable efforts have been made to synthesize titanium nitride with tailored morphology. The design and control of porous structures, nano or mesostructured materials, in which larger specific surface area and more abundant active sites with shorter ion and mass transport distances are expected to further improve its catalytic ability [3]. Thus, the modification of titanium nitride morphology (pore structure and size distribution) has mainly been introduced by ammonolysis using a modified titanium oxide by block copolymers self-assembly. The synthesis of functional materials that include block copolymer self-assembly can create various ordered structures in a wide range of morphologies in materials such as carbon [15,16], oxides [17–19], and nitrides [10,20–22]. Particularly, ordered mesoporous titanium nitride [10] or titanium nitride-carbon nanocomposites [22] have been prepared by employing block copolymers such as poly(ethylene oxide)-block-poly(styrene) and triblock copolymer Pluronic® F127 via ammonolysis.

In this work, titanium nitride is synthesized by a urea-glass process modified with a non-ionic surfactant triblock copolymer Pluronic® F127. In this sense, the solution process allows the easy incorporation of the surfactant (metal-urea complex step) which is further eliminated during heat treatment. Morphology, pore distribution, and bulk and surface chemical composition of titanium nitride particles were investigated. The catalytic activity of the obtained TiN was evaluated for application to oxygen reduction reaction (ORR) catalysts in alkaline conditions because of its interest in electrochemical devices such as metal–air batteries and fuel cells.

Experimental

Chemicals

Titanium chloride ($TiCl_4$, Wako Pure Chemical, 99.0%), 2-methoxy ethanol (2-Me EtOH, Wako Pure Chemical, 98.0%), urea (Wako Pure Chemical, 99.0%), Pluronic® F127 (Sigma–Aldrich), hydrochloric acid (Kanto Chemical, 35%) were used without further purification.

Preparation

Synthesis of TiN by urea-glass process (named as U-TiN)
$TiCl_4$ (metal source) was dissolved in 2-Me EtOH and stirred for 1 h. Urea was added to titanium chloride solution and stirred overnight. The molar ratio of $TiCl_4$ and urea was 1:5. The precursor solution was dried at 80 °C overnight and heated at 3.2 °C min^{-1} under N_2 flow (100 ml min^{-1}) in a tubular furnace up to 800 °C for 3 h. Finally, the furnace was cooled to room temperature to obtain TiN.

Synthesis of TiN by surfactant-modified urea-glass process (named as mU-TiN)
F127 was dissolved in concentrated HCl solution and the solution was added dropwise into the mixture of $TiCl_4$ and 2-Me EtOH (described above). Urea was added to titanium chloride solution containing the surfactant, and then, the mixture was stirred at 80 °C overnight. Subsequent synthesis steps follow the same procedure described above for the U-TiN samples.

Characterization

X-ray diffraction (XRD) patterns were measured using an X-ray diffractometer (Rigaku, MiniFlex 600) with CuKα radiation (λ = 0.15418 nm). The morphology of the samples was observed with Scanning Transmission Electron Microscopy (STEM, Hitachi, HD-2000) and Transmission Electron Microscopy (TEM, JEOL, JEM2010). The surfaces of the powder TiN samples were examined by X-ray Photoelectron Spectrometer (XPS, JEOL, JPS-9200). The surface area and the pore distribution of the samples were determined using N_2 adsorption–desorption analyses (BELSORP-mini). A potentiostat analyser (SI 1287, Solartron) was used for the electrochemical measurements.

Electrochemical characterization

A catalyst suspension was prepared by mixing 1.0 mg of U-TiN or mU-TiN and 300 μL of ethanol (Wako Pure Chemical, 99.5%). The suspension was sonicated for 10 min. Thin-film electrodes on glassy carbon disks (4 mm in diameter) were prepared by dropping (2.0 μL suspension 4 times) and drying (30 min before use). The above procedure yielded a catalyst density loading of 200 μg TiN/cm^2 disk.

Electrochemical measurements were performed using a reported procedure [23]. Briefly, three-electrode setup was used with a rotating disk electrode (RDE) device (BAS, RRDE-3A) as a working electrode, a Hg/HgO electrode as a reference electrode and a Pt electrode as a counter electrode. 1 M KOH solution was used as the electrolyte. The oxygen gas was flowed into the electrolytic solution to induce an oxygen-saturated state for 30 min. Subsequently, linear sweep voltammetry was performed at a scan rate of 5 mV s^{-1} between 0.324 and 1.07 V vs. RHE. The reference potential was converted to the reversible hydrogen electrode (RHE) by applying the Nernst equation [24] and the number of reaction electrons (n) was calculated based on the Koutecky–Levich (KL) equations [25].

Results and discussion

Fig. 1 shows X-ray diffraction (XRD) patterns of U-TiN and mU-TiN sintered at 800 °C. The cubic phase with the $Fm\bar{3}m$ space group (ICSD#64909) was confirmed as the main phase for both materials. The absence of titanium oxide or oxynitrides phases suggests that nitration is occurring from the metal-urea complex. Moreover, the modification of the urea-glass process by adding the surfactant does not affect the formation of the TiN cubic phase.

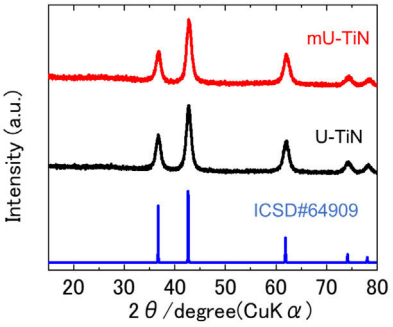

Fig. 1 – XRD patterns of U-TiN and mU-TiN sintered at 800 °C.

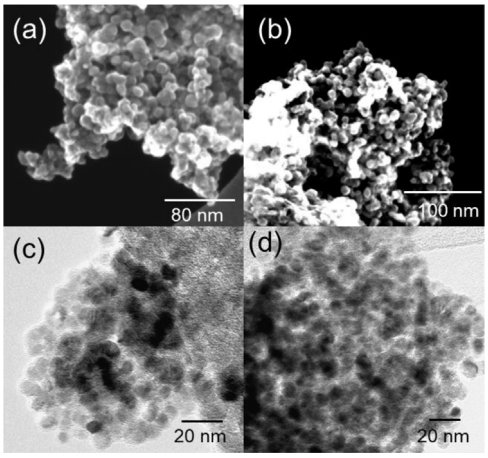

Fig. 2 – SEM images of (a) U-TiN and (b) mU-TiN. TEM images of (c) U-TiN and (d) mU-TiN.

Fig. 2(a) and (b) shows the STEM images of U-TiN and mU-TiN. Both figures show the aggregated morphology of nanoparticles at approximately 10–20 nm. Fig. 2(c) and (d) shows the TEM images of U-TiN and mU-TiN in which single particles with particle sizes of around 5 nm are observed. The modification of the urea-glass process by adding the surfactant hardly affects the morphology of the TiN, maintaining the same particle size and shape.

Fig. 3(a) shows the N_2 adsorption-desorption isotherms of U-TiN and mU-TiN. Both isotherms display typical

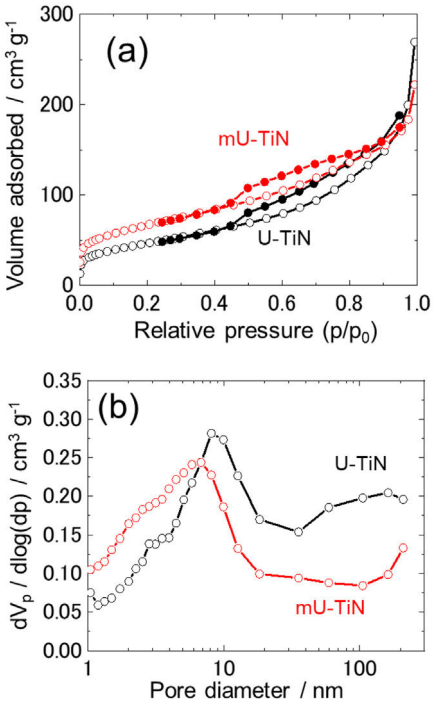

Fig. 3 – (a) N_2 adsorption–desorption isotherm and (b) pore size distribution curves of U-TiN and mU-TiN.

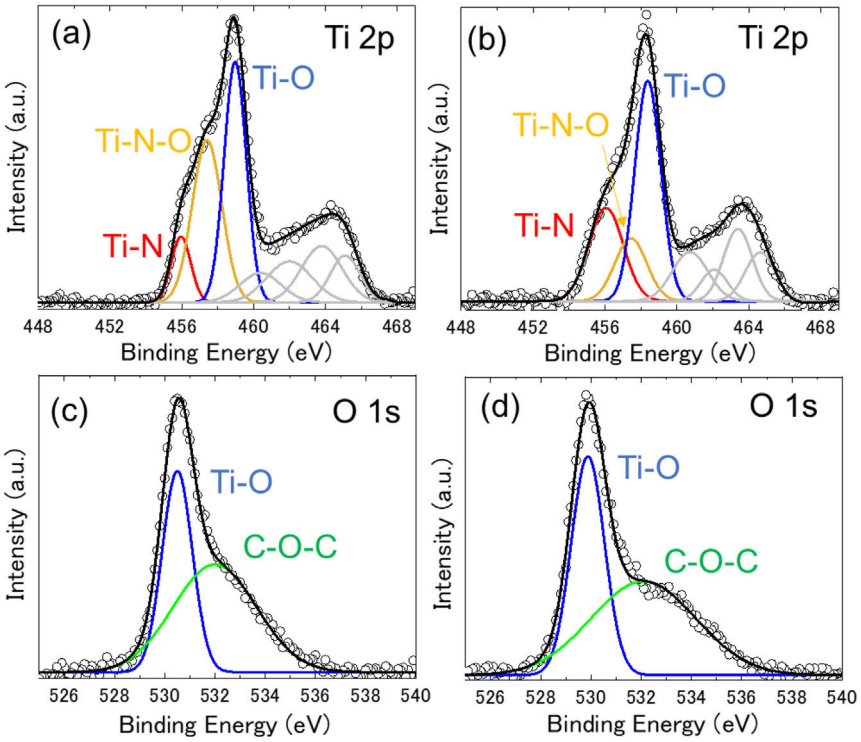

Fig. 4 – Ti 2p XPS spectra of the (a) U-TiN and (b) mU-TiN. Red, yellow and blue lines correspond to Ti—N, Ti—O—N and Ti—O, respectively. Gray lines associated to satellite signals. O 1s XPS spectra of (c) U-TiN and (d) mU-TiN. Blue and green correspond to Ti—O and C—O—C, respectively.

type-IV adsorption isotherm curves with hysteresis loop characteristic of highly mesoporous structures [26]. The specific surface areas of U-TiN and mU-TiN, calculated by Brunauer–Emmett–Teller (BET) theory, were 170 and 240 $m^2 g^{-1}$, respectively. Fig. 3(b) shows the pore distribution curves of U-TiN and mU-TiN obtained by using the Barrett–Joyner–Halenda (BJH) method. The average pore diameter of U-TiN and mU-TiN calculated by BJH analysis was 7.8 nm and 4.8 nm, respectively. From the pore distribution curves, a major mesopore centered at 9 nm diameter is observed for U-TiN while mU-TiN shows two major mesopores centered at 3 and 7 nm diameter, respectively. The modification of the urea-glass process by adding the surfactant reduces the pore diameter maintaining a large surface area.

Fig. 4(a), (b) shows Ti 2p spectra of U-TiN and mU-TiN, respectively. Although the XRD patterns show TiN single phase in both samples, the XPS spectra suggests that their surface can be partially oxidized. Both spectra were deconvoluted with three components assigned to Ti—O (~458 eV), Ti—N—O (~457 eV), and Ti—N (~456 eV) [27], which shows that the chemical states of titanium on the surface of U-TiN and mU-TiN are composed with similar surface chemical composition. However, the intensity ratio of Ti-N/Ti-N-O in mU-TiN component was larger than that of U-TiN, which indicates that the titanium nitride is predominantly distributed on the surface of mU-TiN than that of U-TiN. Fig. 4(c), (d) shows O 1s spectra of U-TiN and mU-TiN, respectively. Both spectra were deconvoluted with two components assigned to Ti—O (~530 eV) and C—O—C (~532 eV) [28]. The C—O—C bond on the surface of U-TiN is associated with the residual carbon species based on urea. In the case of mU-TiN, the C—O—C bond on the surface may also come from the residual carbon species based on surfactant besides urea. Remained carbon species on the surface of the titanium nitride synthesized by the urea-glass method is difficult to remove fully. Carbides and other titanium-carbon subproducts were not found, suggesting that carbon is not reacting with titanium nitride. Moreover, the modification of the urea-glass method by adding the surfactant promotes the formation of a rich nitride layer than oxynitride on the surface of TiN. A possible explanation for this behavior is attributed to a protective role of the surfactant (carbon derivates) that prevent the surface oxidation of the nitrides. The residual carbon or the natural oxidation of surface or reduction of TiO species by carbon residues are expected to have a positive effect on the catalytic activity [29].

Fig. 5(a) shows that oxygen evolution reaction (OER) polarization curves of U-TiN and mU-TiN are comparable. Compared with traditional electrocatalysts such as iridium or other precious metals used in OER [30,31], TiN does not show electroactivity for OER. Fig. 5(b) shows ORR polarization curves of U-TiN and mU-TiN. In contrast to OER, both samples show the ORR catalytic activity comparable to the literature [32]. The mU-TiN exhibits more positive onset potential and larger current density than U-TiN.

Fig. 6 shows Koutecky–Levich plots of U-TiN and mU-TiN corresponding to the rotation rate of 400–2500 rpm at −0.424 V vs RHE. Both plots show linear behavior with estimated elec-

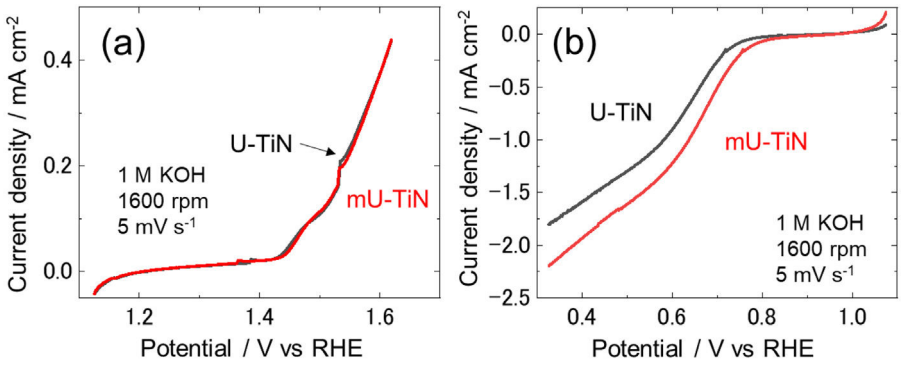

Fig. 5 – (a) OER, (b) ORR polarization curves of U-TiN and mU-TiN measured with a rotating disk electrode in an O_2-sturated 1 M KOH solution at a scan rate of 5 mV s^{-1}.

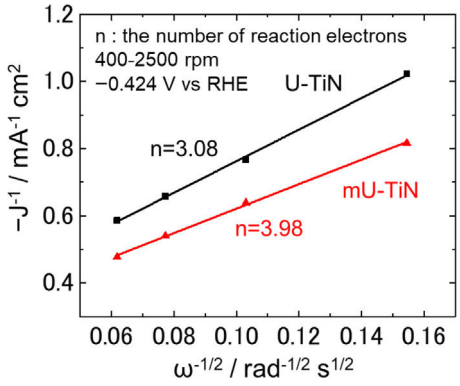

Fig. 6 – Koutecky–Levich plots of U-TiN and mU-TiN at −0.424 V vs RHE and 400–2500 rpm. *n* indicates the number of reaction electrons measured at 400–2500 rpm at −0.424 V vs. RHE.

tron transfer numbers (Eq. (2)) of 3.08 and 3.98 for U-TiN and mU-TiN, respectively.

The electron transfer number of U-TiN (3.08) is in close agreement with the previously reported number of carbon-coated TiN nanoparticles (2.92) [33,34]. In this case, the ORR on U-TiN may proceed by a coexisting pathway involving both the two-electron and four-electron transfers (Eqs. (1)–(3)).

$$O_2 + H_2O + 4e^- \rightarrow 4OH^- \quad (1)$$

$$O_2 + H_2O + 2e^- \rightarrow HO_2^- + OH^- \quad (2)$$

$$HO_2^- + H_2O + 2e^- \rightarrow 3OH^- \quad (3)$$

Interestingly, the ORR on mU-TiN proceeds by almost four-electron transfers (Eq. (3)). This result is of particular interest since the formation of intermediates in two-electrons processes can be prevented. Because chemical composition of nitrides changes the electronic structures and the residual carbon can work as the catalytic active sites, the enhanced catalytic ability is interpreted as a result of different surface modification of titanium nitride, shown in Fig. 4, obtained by the surfactant-modified urea-glass process.

Conclusions

Titanium nitride was synthesized by a urea-glass method with and without surfactant Pluronic® F127. Regardless of surfactant use, the formation of TiN nanoparticles with a size of circa 5 nm was confirmed. Mesostructured TiN with a smaller pore diameter and largest surface area is obtained by the surfactant-modified urea-glass method. The surface chemical composition of titanium nitride shows the presence of titanium oxide, titanium oxynitride and residual carbon. However, a relative higher nitride/oxynitride layer was obtained by the surfactant-modified urea-glass method. ORR catalytic activity can be enhanced to a four-electron transfer when TiN is obtained by surfactant-modified urea-glass method.

Authors' contributions

Y.S. and S.I. have conducted experiments. Y.S. wrote the first draft. N.C.R.-N., A.M. and K.T. supervised the work. All authors have revised and edited the final version of the manuscript.

Ethical approval

Not applicable.

Funding

This research was supported by EIG CONCERT-Japan 4th Call under the Strategic International Collaborative Research Program (SICORP) of the Japan Science and Technology Agency (JST).

Conflict of interests

Not applicable.

Availability of data and materials

The experimental section includes a complete description of materials and sources to reproduce the procedures reported in this work. Data reported correspond to an average behavior of at least three measures.

Acknowledgments

This research was supported by EIG CONCERT-Japan 4th Call under the Strategic International Collaborative Research Program (SICORP) of the Japan Science and Technology Agency (JST).

REFERENCES

[1] C. Hu, K. Guo, Y. Li, Z. Gu, J. Quan, S. Zhang, W. Zheng, Thin Solid Films 688 (2019) 137339.
[2] S. Seal, JOM 53 (2001) 51–54.
[3] H. Wang, J. Li, K. Li, Y. Lin, J. Chen, L. Gao, V. Nicolosi, X. Xiao, J.M. Lee, Chem. Soc. Rev. 50 (2021) 1354–1390.
[4] Y. Zheng, X. Li, C. Pi, H. Song, B. Gao, P.K. Chu, K. Huo, FlatChem 19 (2020) 100149.
[5] M.S. Balogun, Y. Huang, W. Qiu, H. Yang, H. Ji, Y. Tong, Mater. Today 20 (2017) 425–451.
[6] H. Pan, Mater. J. Chem. A 3 (2015) 21486–21493.
[7] Y.J. Wang, D.P. Wilkinson, J. Zhang, Chem. Rev. 111 (2011) 7625–7651.
[8] W.F. Chen, J.T. Muckerman, E. Fujita, Chem. Commun. 49 (2013) 8896–8909.
[9] J.G. Chen, Chem. Rev. 96 (1996) 1477–1498.
[10] B.G. Kim, C. Jo, J. Shin, Y. Mun, J. Lee, J.W. Choi, ACS Nano 11 (2017) 1736–1746.
[11] B. Avasarala, T. Murray, W. Li, P. Haldar, J. Mater. Chem. 19 (2009) 1803–1805.
[12] N.F. Daudt, A. Poozhikunnath, H. Yu, L. Bonville, R. Maric, Mater. Renew. Sustain. Energy, doi:10.1007/s40243-020-00179-1.
[13] J. Li, L. Gao, J. Sun, Q. Zhang, J. Guo, D. Yan, J. Am. Ceram. Soc. 84 (2001) 3045–3047.
[14] C. Giordano, C. Erpen, W. Yao, B. Milke, M. Antonietti, Chem. Mater. 21 (2009) 5136–5144.
[15] Y. Meng, D. Gu, F. Zhang, Y. Shi, H. Yang, Z. Li, C. Yu, B. Tu, D. Zhao, Angew. Chem.-Int. Ed. 44 (2005) 7053–7059.
[16] C. Liang, K. Hong, G.A. Guiochon, J.W. Mays, S. Dai, Angew. Chem.-Int. Ed. 43 (2004) 5785–5789.
[17] M. Templin, A. Franck, A. Du Chesne, H. Leist, Y. Zhang, R. Ulrich, V. Schädler, U. Wiesner, Science (80-) 278 (1997) 1795–1798.
[18] D. Zhao, J. Feng, Q. Huo, N. Melosh, G.H. Fredrickson, B.F. Chmelka, G.D. Stucky, Science (80-) 279 (1998) 548–552.
[19] K.W. Tan, H. Sai, S.W. Robbins, J.G. Werner, T.N. Hoheisel, S.A. Hesse, P.A. Beaucage, F.J. Disalvo, S.M. Gruner, M. Murtagh, U. Wiesner, RSC Adv. 5 (2015) 49287–49294.
[20] M. Maleki, A. Beitollahi, J. Lee, M. Shokouhimehr, J. Javadpour, E.J. Park, J. Chun, J. Hwang, RSC Adv. 5 (2015) 6528–6535.
[21] S.W. Robbins, H. Sai, F.J. Disalvo, S.M. Gruner, U. Wiesner, ACS Nano 8 (2014) 8217–8223.
[22] E. Ramasamy, C. Jo, A. Anthonysamy, I. Jeong, J.K. Kim, J. Lee, Chem. Mater. 24 (2012) 1575–1582.
[23] Y. Iwai, A. Miura, C. Rosero-Navarro, M. Higuchi, K. Tadanaga, J. Asian Ceram. Soc. 7 (2) (2019) 147–153.
[24] S. Brocato, C. Lau, P. Atanassov, Electrochim. Acta 61 (2012) 44–49.
[25] J. Qiao, L. Xu, P. Shi, L. Zhang, R. Baker, J. Zhang, Int. J. Electrochem. Sci. 8 (2013) 1189–1208.
[26] J. Yuan, Z. Liu, Y. Wen, H. Hu, Y. Zhu, V. Thangadurai, Ionics (Kiel.) 25 (2019) 1669–1677.
[27] S. Jiang, B. Yi, H. Zhang, W. Song, Y. Bai, H. Yu, Z. Shao, ChemElectroChem 3 (2016) 734–740.
[28] G. Zorn, V. Migonney, D.G. Castner, Biointerphases 9 (2014) 031001.
[29] Y. Yao, R. Zeng, Y. Xiong, F.J. DiSalvo, H.D. Abruña, J. Am. Chem. Soc 141 (49) (2019) 19241–19245.
[30] A. Lončar, D. Escalera-López, S. Cherevko, N. Hodnik, Angew. Chem. Int. Ed. 61 (14) (2022), e202114437.
[31] Q. Wang, C. Xu, W. Liu, S. Hung, H. Bin Yang, J. Gao, W. Cai, H. Chen, J. Li, B. Liu, Nat. Commun. 11 (1) (2020) 4246.
[32] X. Ge, et al., ACS Catal. 5 (8) (2015) 4643–4667.
[33] J. Chen, X. Wei, J. Zhang, Y. Luo, Y. Chen, G. Wang, R. Wang, Ind. Eng. Chem. Res. 58 (2019) 2741–2748.
[34] Y. Dong, Y. Wu, M. Liu, J. Li, ChemSusChem 6 (2013) 2016–2021.